# REEL Demo – Romande Energie ELectric network in local balance Demonstrator

## Deliverable: 5b Design of sizes for buildings energy systems as a function of the grid evolution

## Demo site: Rolle

Developed by
Luise MIDDELHAUVE (EPFL-IPESE)
Lionel BLOCH (EPFL-PVlab)
Luc GIRARDIN (EPFL-IPESE)
in collaboration with
Paul STADLER (EPFL-IPESE)
Jordan HOLWEGER (EPFL-PVlab)
Hervé TOMMASI (EPFL-IPESE)

[Sion/Neuchâtel, 27.06.2018]

# Contents

# Nomenclature

ACRONYMS

| | |
|---|---|
| $CAPEX$ | Capital Expenditure |
| $ELDC$ | Error in Load Duration Curve |
| $EMS$ | Energy Management Systems |
| $GIS$ | Geographic Information System |
| $GM$ | Grid Multiple |
| $LPEM$ | Low temperature Proton Exchange Membrane fuel cells |
| $LV$ | Low Voltage |
| $MAE$ | Mean Absolute Error |
| $MILP$ | Mixed integer linear programming |
| $MPC$ | Model Predictive Control |
| $MRAE$ | Mean Relative Absolute Error |
| $MSE$ | Mean Squared Error |
| $MV$ | Medium Voltage |
| $OPEX$ | Operational Expense |
| $PE$ | Percentage Error |
| $PRAE$ | Peak Relative Absolute Error |
| $PV$ | Photovoltaic |
| $SOFC$ | Solid Oxide Fuel Cells |
| ERA | Energy reference area |
| SC | Self-consumption |
| SS | Self-suciency |

SYMBOLS

| | |
|---|---|
| $\dot{E}_b^-$ | Building uncontrollable load profile |
| $\dot{E}_{grid}$ | Power profile to/from the grid |
| $\epsilon_I$ | Investment cost $\epsilon$-constraint |
| $\epsilon_{GM}$ | Grid Multiple $\epsilon$-constraint |
| $A$ | Area |
| $d_p$ | Period duration |
| $d_t$ | Timestep duration |
| $E$ | Electrical energy |
| $f_u$ | Unit size factor |
| $F_u^{max}$ | Device maximal sizing values |
| $F_u^{min}$ | Device minimal sizing values |
| $H$ | Chemical gas–power flows |
| $I_{1,u}$,$I_{2,u}$ | Investment cost parameters [CHF, CHF/m] |
| $N$ | Project horizon |
| $n$ | Total number |
| $N_u$ | Unit lifetime |
| $op$ | Grid energy tariffs |
| $Q$ | Thermal energy |
| $Q_{u_c}^+$ | Heat demand of utility ($u_c$) |
| $Q_{u_h}^-$ | Released heat of utility ($u_h$) |
| $R$ | Heat cascade residual |
| $r$ | Project interest rate |
| $rep_u$ | unit purchases over $N$ |
| $s$ | Silhouette coefficient |
| $T$ | Temperature [K] |
| $u_c$ | Cold utility |
| $u_h$ | Hot utility |
| $y_u$ | Unit existence |

| | |
|---|---|
| $y_{u,p,t}$ | Logical state on/off of unit $u$ |
| SETS | |
| B | Building |
| K | Temperature level |
| P | Period (day) |
| T | Time (hour) |
| U | Utility types |
| $\Sigma$ | Decision variables |
| SUBSCRIPTS/SUPERSCRIPTS | |
| $+/-$ | Incoming/outgoing flow |
| $amb$ | Ambient |
| $b$ | Building |
| $c$ | Cooling |
| $cl$ | Cluster |
| $d$ | Day |
| $el$ | Electrical |
| $grid$ | Electrical grid or thermal network |
| $h$ | Heating |
| $k$ | Heat cascade interval index |
| $p$ | Operating period (typical day) |
| $t$ | Time (hour) |
| $u$ | Unit, device |

# 1. Description of deliverable and goal

## 1.1. Executive summary

The increasing use of renewable energy is a deep going trend mainly supported by the sustained annual growth rate of solar photovoltaic, wind power and biogases.
The expansion and evolution of the distribution grids is therefore a key issue to ensure a secure and sustainable supply of electricity in the future.

This report presents an integrated approach for the elaboration of alternative scenarios for the future grid evolution. The proposed method allows to optimally design and schedule building energy systems within the context of smart grids. It combines geographical information system, process integration techniques and power flow analysis to model the holistic district energy system including heat cascading and network constraints to ensure power quality. The scenarios at district scale results form the aggregation of optimal energy technology configurations at building scale given as a function of the investment capacity. This approach therefore allows to evaluate the effect of the increase of prosumer capacities in the grid.

## 1.2. Research question

In May 2017, the Swiss population approved the government Energy Strategy 2050, thus progressively inducing a major transition from a classical top-down electricity generation to a more prosumers-centered approach combined with a nuclear energy phase-out [8]. This decentralized electricity generation, whose growth is partly due to PV installations at the European level, might however generate market congestion due to unfriendly deployment and operation within the electrical grid [15], thus inducing an increased flexibility need.

This flexibility issue has been the center of interest of both industrial stakeholders and research institutes. Indeed, solutions based on prosumers flexibility, smart grids and buildings as well as multi-energy systems optimal planning and operation offer insights into cost effective solutions for renewable energy integration. Model Predictive Control (MPC) applied to smart buildings alone is estimated to provide up to 8.7 [GWh] equivalent battery capacity at the Swiss level [11].

Combining the conflicting needs for renewable energy integration and safe grid operation, the work-package 5 of SCCER-FURIES: ReEL aims at providing recommendations for sizing and operations of buildings multi-energy systems for renewable integration in the optic of the Swiss energy transition.

## 1.3. Novelty of the proposed solutions compared to the state-of-art

A novel approach is presented to optimally design and schedule building energy systems within the context of smart grids. Indeed, the active management of heterogeneous dwelling loads connected to a single feeder represents an interesting solution to the improve the integration of distributed and renewable energy sources in neighbourhoods.
The proposed method uses mixed integer linear programming (MILP) techniques to model the holistic building energy system structure which includes heat cascading and network constraints to ensure power quality. Once the building energy system has been optimaly defined, its impact on the grid is analyzed using a state-of-the art power flow algorithm.

## 1.4. Description

This deliverable present the methodology and results of the optimal planning and operation of buildings multi-energy systems, taking into account the electrical grid safe operation. This deliverable is the result of the common work between EPFL - IPESE and EPFL - PV-lab in order to combine the knowledge to produce the most accurate results.

The general approach consists in developing smart buildings optimization models based on actual field data, and then to design and operate the system according to an MILP-based optimization procedure. The optimization objectives are defined according to scenarios taking into account capital expenses and renewable energy integration, and results are used to simulate the grid, identify limitations and possible problems occurring during grid operation.

In a first instance, the building-sector-related electrical grid challenges are presented in a global vision of renewable energy in Europe and Switzerland (section 4).

In a second instance, the methodology is detailed in 6 phases undertaken to produce the hereafter presented results (section 5), before detailing the geographical and temporal data reduction (section 6) as well as building multi-energy systems modeling (section 7).

In a third instance, optimization results for a single building (section 8) is presented and interpreted both in terms of performance indicators (capital expenses and renewable energy share) and chosen building technologies. The results are then used as inputs for grid simulations and the corresponding impacts are assessed (section 9).

Finally, the upcoming steps of the SCCER-FURIES: REeL research project as well as insights in future research developments are presented in section 10.

# 2. Achievement of Deliverable

## 2.1. Date

This deliverable is handed in June 2018.

## 2.2. Demonstration of the Deliverable

The deliverable capitalizes on previously published research developments of EPFL-IPESE and EPFL-PV-lab, new research and data provided both by public organs and industrial partners.

# 3. Impact

The impact of this project is to provide technical recommendations for technologies assessment and optimal renewable energy integration to an industrial partner and thus further influence his decisions for upcoming investment in western Switzerland. Furthermore, this project has been the opportunity to strengthen the links between researchers from both EPFL and other research institutes.

### Main Publications

[MP1] Araz Ashouri, Paul Stadler, and François Maréchal. Day-ahead promised load as alternative to real-time pricing. In Smart Grid Communications (SmartGridComm), 2015 IEEE International Conference on, pages 551–556. IEEE, 2015.

[MP2] Nils Schüler, Sébastien Cajot, Markus Peter, Jessen Page, and François Maréchal. The optimum is not the goal Capturing the decision space for the planning of new neighborhoods. Frontiers in Built Environment - Urban Science, August 2017.

[MP3] P. Stadler, L. Girardin, and F. Marechal. The Swiss Potential of Model Predictive Control for Building Energy Systems”. 2017.

[MP4] Paul Stadler, Araz Ashouri, and François Maréchal. Model-based optimization of distributed and renewable energy systems in buildings. 120:103–113, 2016.

[MP5] Paul Stadler, Araz Ashouri, and François Maréchal. Distributed model predictive control of energy systems in microgrids. In Systems Conference (SysCon), 2016 Annual IEEE, pages 1–6. IEEE, 2016.

[MP6] Paul Stadler, Luc Girardin, Araz Ashouri, and François Maréchal. Contribution of Model Predictive Control in the Integration of Renewable Energy Sources within the Built Environment. Frontiers in Energy Research, 6, May 2018.

# 4. Electrical Grid Challenges for Optimal Stochastic Renewable Energy Integration in the Building Sector

Over the last decade, the massive deployment of renewable energy for both heat and electricity generation in Europe represents a increasing trend indicating towards an fundamental energy transition [15]. Indeed, most European Union (EU) countries have been increasing their renewable energy share since 2005, and objectives for 2020 indicate an continuous rise (see Figure 1):

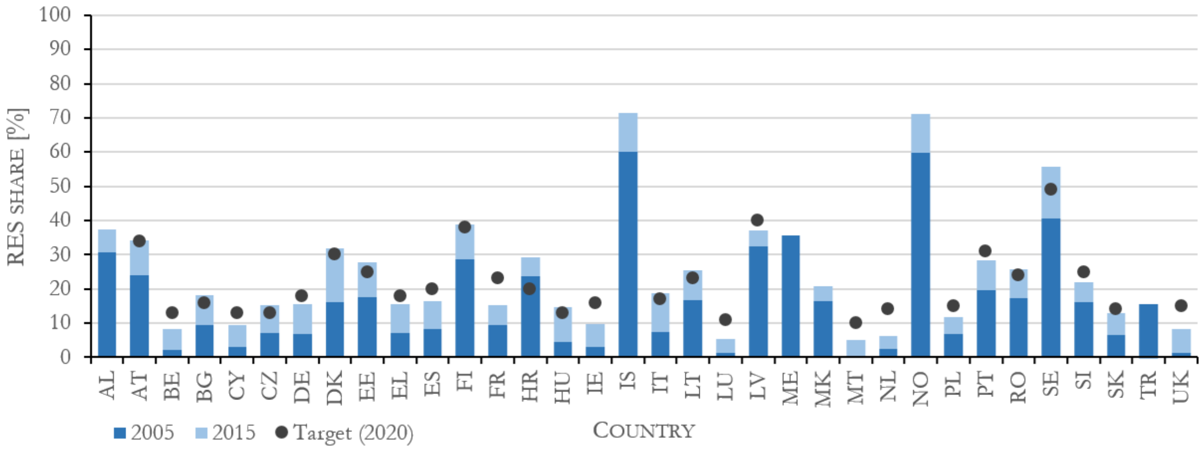


Figure 1: RES Share in Gross Final Energy Consumption for EU [3]

The corresponding short- (2020) and mid-term (2030) intermediary objectives towards a resource-efficient European society are consistent with the Swiss population vote for the 2050 Energy Strategy [8]. In facts, it is translated by a common trend of increasing stochastic renewable energy sources integration in the energy mix. Indeed, in the case of solar photovoltaic energy generation, the trend is even more pronounced both for the main European Union stakeholders as well as for Switzerland (see Figure 2), with an exponential-like increase both for the absolute and renewable energy share values (hydropower excluded).

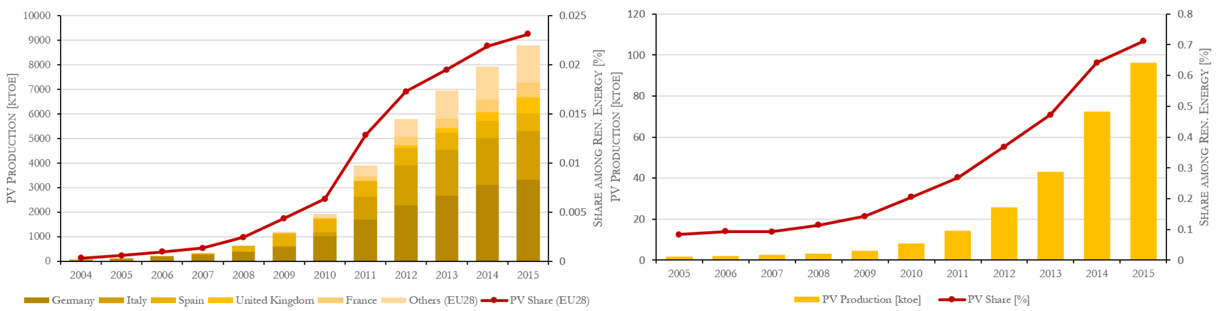


(a) European Union

(b) Switzerland

Figure 2: PV energy generation of the major European stakeholders and Switzerland and its share in the renewable energy production (hydropower excluded) [3, 5]

This renewable increase trend follows the Swiss government 3 axis for a successful energy transition: increase the energy efficiency of systems, augment renewable energy use and and progressively withdraw from nuclear energy [8]. Among the targeted sectors to undergo an increase of energy efficiency, buildings are the one combining the increase for renewable energy use due to their roof solar potential, and are therefore subject to government-supported investments through building programs and tax deduction [8]. In order to orient these investments, researches in the field of urban planning based on parametric optimization and mixed-integer linear programming models have been proven to be successful tools for planning of urban districts including renewable energy sources [MP2].

Furthermore, new technologies and researches are proposing innovative solutions for non-controllable and stochastic load profiles risk minimization, such as Energy Management Systems (EMS) applied to Model Predictive Controlled (MPC) smart buildings, both for the operation [MP5, MP1] and design of such systems [1][12]. Inclusion of smart systems into the grid are also to play an important role in the Swiss energy transition, as legal basis for the introduction of smart solutions such as smart metering are part of the Swiss energy strategy 2050 [8].

In this transition context with PV, buildings and smart systems orientations, the need for a cost-efficient and technically coherent renewable energy integration is of main concern for grid operators. Indeed, optimal design and grid-friendly operation (with self-consumption maximization) is necessary to avoid hampering the PV market due to grid operation issues [15]. Therefore, the SCCER-FURIES: REeL fifth workpackage aims at combining the knowledge from different research entities and industrial partners in the optic of creating an efficient methodology and the corresponding tool for renewable energy integration in the building sector, thus contributing to the undertaken Swiss energy transition.

# 5. Research Methodology

The research methodology has been developed in the optic of producing a method for optimal renewable energy integration easily transposable to other study cases in Switzerland. Therefore, an automated GIS-based tool was developed to combine existing building and energy systems databases with RE[1] grid data and automatically produce results.

## 5.1. Data Collection and Compilation

The first phase of the methodology consists in data collection and compilation. Data has been selected based on multiple qualitative criteria:

- They have to include both thermal, electrical and environmental data for an optimal assessment of all possibilities and technologies.
- Due to the opportunity of an actual demonstrator, real data has to be favored over simulated ones.
- Data available over all Switzerland is favored for a relocatable/scalable approach. If data has to be localized, the Rolle demonstrator location is preferred.
- As illustrated in section 4, the integration of PV installations in Europe follows an increasing trend. Therefore, up-to-date results are selected for the sake of results coherency.

Data, due to its verified provenance, is supposed to be correct. Its completeness is however assessed and taken into account for geographical clustering (section 6.1) and results interpretation. The complete presentation of data collection and compilation has already been presented in another project, SCCER-FURIES: JA-RED.

## 5.2. Geographical and Temporal Clustering

In order to reduce the computational tasks to be undertaken during the optimization phase, geographical and temporal clustering is applied to the project data.

Geographical clustering is based on the division into LV grid associated buildings, and each cluster is assessed through a combination of quantitative criteria combined with a double-weighted decision matrix. The selection of one LV-grid associated buildings allows to reduce the number of building-related computations to be done.

In parallel, temporal clustering is performed based on significant meteorological data: outside temperature and global irradiation. This approach allows to reduce the number of periods to be considered

[1]Main industrial partner Romande Énergie

and therefore the computational burden.

Both approaches are further detailed in section 6.

## 5.3. Building and Energy Systems Modeling

The building and energy systems modeling is done based on a formulation allowing to consider the optimization problem as a Mixed-Integer Linear Programming (MILP) problem. The models considered are to remain simple in order to allow multiple buildings impact assessment:

- The dynamic building model follows a linear one degree of freedom RC-based structure.
- The energy systems models are adapted according to the technology considered, but remain black-box-based and static for most of them

The modeling of the building and its energy systems are detailed in section 7.

## 5.4. Single Building Optimization

The single building modeling allows to focus on a single element from the preselected LV-grid cluster in order to present and interpret the building behavior and technologies choices/sizing in a detailed way.

The generation of local Pareto curves representing the trade-off between opposing objectives, such as renewable energy integration and capital expenses, as well as the presentation of the technologies associated to each building scenario and their corresponding interpretation are the objectives of this step, as detailed in section 8.

## 5.5. Buildings/District to Grid-impact Assessment

Optimization performed on the various buildings connected amongst a LV grid leads to a set of similar results than the ones presented in the previous methodology step. However, their aggregation at various levels (building, LV and MV transformer) allows to generate multiple curves and technologies choices that represent the diversity in terms of building ages, purposes and sizes.

Furthermore, the grid simulation for the selected scenarios allows to assess the impact on existing electrical infrastructure and to identify critical points for future grid planning. These two aspects are further detailed in section 9.

## 5.6. Investment for Renewable Energy Integration

The outcome of this methodology is to present recommendations for optimal integration of renewable energy into the built environment as well as to produce a automated GIS-based tool in order to easily translate the methodology into another context. The resulting recommendations are to be detailed in future research reports ”Final report on the planning of multi-energy systems” to be submitted before 31 December 2020

.

# 6. Geographical and Temporal Data Reduction

Optimization of multi-energy systems represents a challenge in terms of computational limits due to the size of the implemented optimization problem. Indeed, the computational burden might lead to prohibitive computation time. To remedy to this issue, clustering has been highlighted as an efficient solution while maintaining results coherency [4][12].

In this project, two independent clustering have been chosen: one based on LV-grid related geographical data (section 6.1), and another one based on irradiation and temperature-related temporal data (section 6.2).

## 6.1. Grid-defined Geographical Clusters

The first clustering based on geographical data follows the technical boundaries defined by the grid data provided by the main industrial partner. Indeed, in order to be coherent with a grid-centered approach, buildings are divided into groups associated with the corresponding transformer. Based on these predefined clusters (see Figure 3), a selection of criteria were evaluated and a ranking according to these performance criteria was done. Then, in order to take into account both data completeness and each criterion importance, two types weighting factors were introduced. The final ranking was done by the minimal value among the LV grids.

It is important to notice that, due to the main industrial partner interests, the low voltage grid selection range was restricted to 6 predefined LV grids: BOURDONNETTE-TR4178, BOURGEOISES-TR4756, GARE-TR4513, HÔPITAL-TR3716, MARTINET-TR4769 and RTE DE LA PRAIRIE-TR7575.

An example of evaluated criterion for the selected low voltage grids is the building solar potential for both all and only well-oriented roofs, as illustrated in Figure 4.

The final matrix summarizing the ranking is available in Table 1, therefore indicating the quantitative choice of the LV-grid reference as the one associated to the HOPITAL-TR3716 transformer. This approach has already been applied and documented within the JA-RED project, as the corresponding report thoroughly details the criteria assessment and is therefore set as reference for more information.

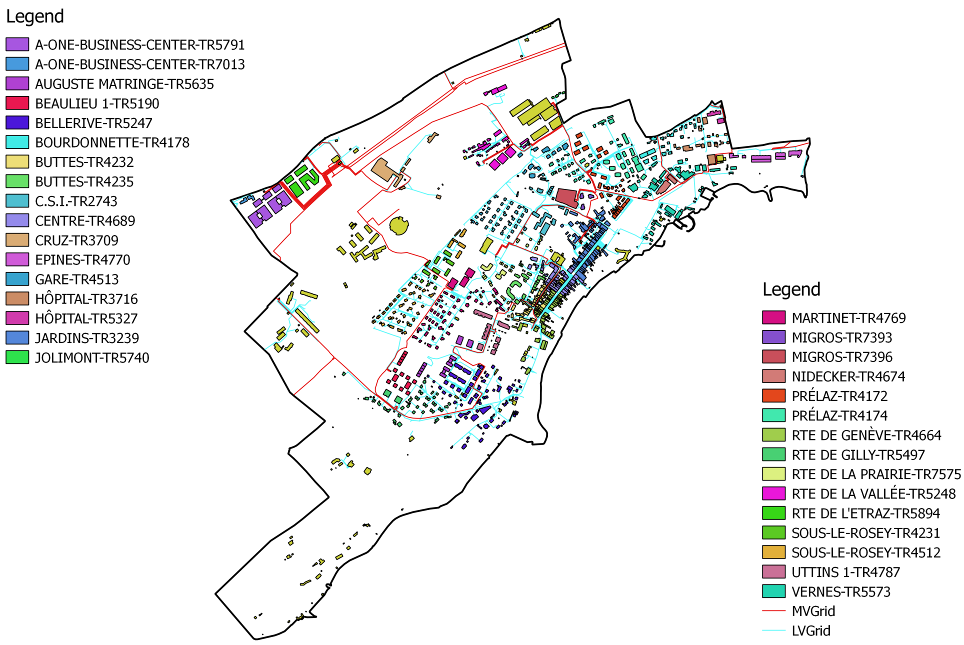


Figure 3: Geographical repartition of transformer-allocated buildings in Rolle (JA-RED project)

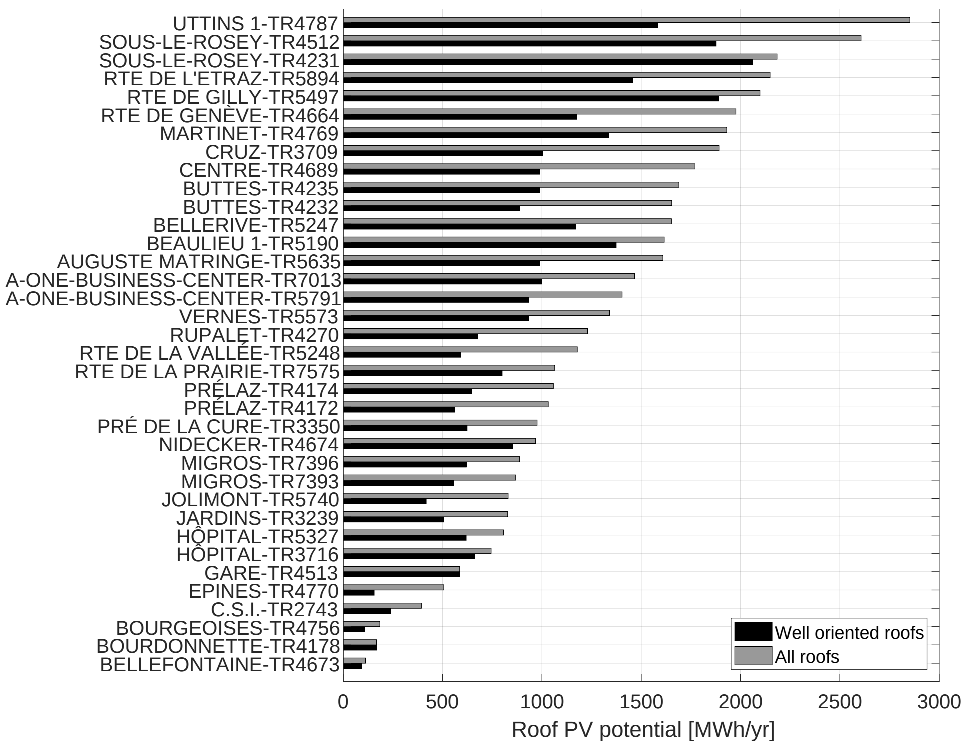


Figure 4: Ordered roof PV potential aggregated per LV-transformer (JA-RED project)

| LV Grid | Buildings | | | Thermal Energy | | Electricity | Penalty |
|---|---|---|---|---|---|---|---|
| | Age | SRE | Purpose | Heating Sys. | Thermal Pow. | Solar Pot. | |
| A-ONE-BUSINESS-CENTER-TR5791 | 36 | 3 | 31 | 21 | 24 | 2 | 232.63 |
| A-ONE-BUSINESS-CENTER-TR7013 | 12 | 13 | 13 | 28 | 36 | 36 | 238.87 |
| AUGUSTE MATRINGE-TR5635 | 35 | 11 | 11 | 32 | 26 | 24 | 252.35 |
| BEAULIEU 1-TR5190 | 30 | 28 | 32 | 33 | 21 | 22 | 326.63 |
| BELLEFONTAINE-TR4673 | 23 | 7 | 29 | 27 | 2 | 4 | 206.76 |
| BELLERIVE-TR5247 | 13 | 16 | 15 | 10 | 7 | 3 | 128.70 |
| BOURDONNETTE-TR4178 | 29 | 33 | 23 | 24 | 18 | 5 | 255.40 |
| BOURGEOISES-TR4756 | 22 | 29 | 21 | 1 | 22 | 17 | 203.48 |
| BUTTES-TR4232 | 9 | 23 | 12 | 18 | 19 | 20 | 182.73 |
| BUTTES-TR4235 | 6 | 21 | 25 | 22 | 28 | 28 | 241.34 |
| C.S.I.-TR2743 | 20 | 25 | 3 | 16 | 15 | 6 | 148.90 |
| CENTRE-TR4689 | 3 | 14 | 16 | 7 | 4 | 11 | 113.96 |
| CRUZ-TR3709 | 14 | 8 | 18 | 31 | 8 | 8 | 181.10 |
| EPINES-TR4770 | 16 | 2 | 4 | 12 | 6 | 26 | 122.74 |
| GARE-TR4513 | 4 | 20 | 14 | 3 | 27 | 25 | 156.50 |
| HÔPITAL-TR3716 | 24 | 15 | 7 | 4 | 3 | 9 | 118.96 |
| HÔPITAL-TR5327 | 19 | 12 | 9 | 35 | 29 | 34 | 244.81 |
| JARDINS-TR3239 | 2 | 17 | 5 | 20 | 1 | 1 | 94.26 |
| JOLIMONT-TR5740 | 34 | 34 | 28 | 25 | 31 | 27 | 333.19 |
| MARTINET-TR4769 | 21 | 26 | 10 | 6 | 16 | 12 | 161.96 |
| MIGROS-TR7393 | 32 | 35 | 36 | 36 | 33 | 35 | 393.98 |
| MIGROS-TR7396 | 15 | 1 | 30 | 30 | 17 | 21 | 233.58 |
| NIDECKER-TR4674 | 33 | 36 | 35 | 34 | 34 | 32 | 385.95 |
| PRÉ DE LA CURE-TR3350 | 27 | 32 | 34 | 2 | 30 | 23 | 275.01 |
| PRÉLAZ-TR4172 | 11 | 9 | 20 | 5 | 13 | 14 | 140.59 |
| PRÉLAZ-TR4174 | 10 | 10 | 17 | 9 | 5 | 10 | 126.66 |
| RTE DE GENÈVE-TR4664 | 1 | 22 | 8 | 19 | 10 | 15 | 139.93 |
| RTE DE GILLY-TR5497 | 17 | 30 | 2 | 14 | 23 | 19 | 174.53 |
| RTE DE LETRAZ-TR5894 | 8 | 5 | 33 | 11 | 32 | 31 | 224.69 |
| RTE DE LA PRAIRIE-TR7575 | 18 | 27 | 26 | 26 | 25 | 29 | 285.40 |
| RTE DE LA VALLÉE-TR5248 | 7 | 18 | 6 | 23 | 14 | 7 | 136.85 |
| RUPALET-TR4270 | 28 | 24 | 24 | 13 | 35 | 33 | 280.65 |
| SOUS-LE-ROSEY-TR4231 | 26 | 6 | 27 | 15 | 20 | 30 | 240.12 |
| SOUS-LE-ROSEY-TR4512 | 25 | 31 | 22 | 8 | 12 | 16 | 220.44 |
| UTTINS 1-TR4787 | 31 | 4 | 19 | 29 | 11 | 18 | 225.14 |
| VERNES-TR5573 | 5 | 19 | 1 | 17 | 9 | 13 | 113.56 |
| Completeness Indicator | 0.95 | 0.87 | 0.95 | 0.73 | 0.87 | 0.59 | |
| Criteria Weight | 2 | 2 | 3 | 3 | 1 | 3 | |

Table 1: Double-weighted decision matrix for the subsystem selection (JA-RED project)

## 6.2. Temperature and Irradiation-based Temporal Clusters

As detailed in [4], temporal clustering based on decision variables like temperature and irradiation is an efficient way to reduce the number of data and thus the computational burden. However, as highlighted in [12], a k-medoids approach is preferred. The clustering quality is assessed in two different ways: graphically, through the coherency between the load curves of both the temperature and the irradiation, and quantitatively through the following indicators for each clusters number $cl$, similarly to [12] and [9]:

- The silhouette coefficient $s$, which should be above the consistency threshold of 0.25 and if possible above 0.5, the higher value the better.
- The Mean Squared Error $MSE$, to be minimized
- The Mean Absolute Error $MAE$, to be minimized
- The Percentage Error $PE$, to be minimized as an absolute value
- The Mean Relative Absolute Error $MRAE$ [%], to be minimized for each variable
- The Peak Relative Absolute Error $PRAE$ [%], to be minimized for each variable

The clustering is done based on an individual time range of one day from 12 a.m. to 23 p.m., with a corresponding time-step of 1 hour, similarly to [12]. The corresponding load curves for temperature/global irradiation with a cluster number $n_{cl}$ of 10 are displayed in Figure 5, and the indicators for a cluster number $n_{cl}$ from 8 to 12 are summarized in Table 2. As observed, the latter graph provides a visual validation of the selected clusters [9, 14].

| Global Indicators | | | | | Temperature | | Irradiation | |
|---|---|---|---|---|---|---|---|---|
| $cl$ | $s$ | $MSE$ | $MAE$ | $PE$ | $MRAE$ | $PRAE$ | $MRAE$ | $PRAE$ |
| 8 | 0.43 | 0.24 | 2.18 | -0.80 | 5.23 | 21.90 | 3.87 | 55.57 |
| 9 | 0.42 | 0.22 | 2.09 | -2.10 | 4.84 | 23.22 | 3.89 | 55.38 |
| 10 | 0.42 | 0.21 | 2.01 | -7.23 | 4.70 | 19.79 | 3.68 | 55.09 |
| 11 | 0.39 | 0.20 | 1.95 | -8.17 | 4.51 | 19.26 | 3.61 | 55.38 |
| 12 | 0.39 | 0.19 | 1.89 | -5.90 | 4.51 | 20.32 | 3.38 | 56.23 |

Table 2: Outside temperature and global irradiation clustering performance indicators

Considering the previously detailed criteria, the best trade-off between computational burden reduction and clustering performance is represented by a cluster number of 10, and is therefore taken as temporal basis for the upcoming optimizations.

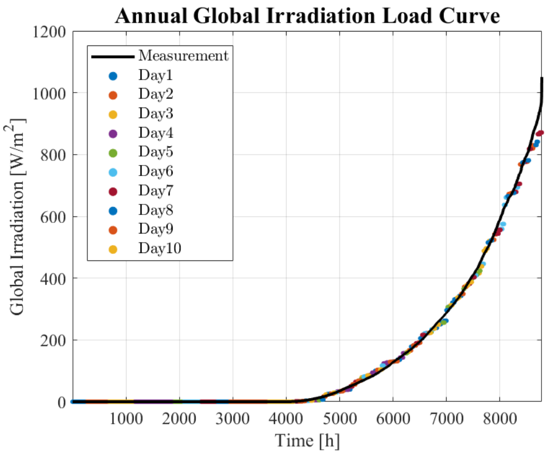


(a) Outside temperature load curve

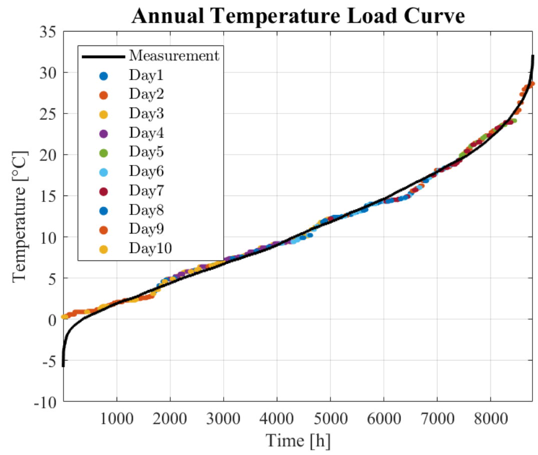


(b) Global irradiation load curve

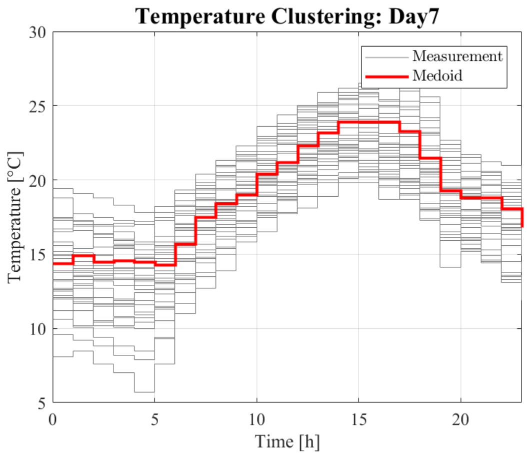


(c) Example temperature cluster for typical day 7

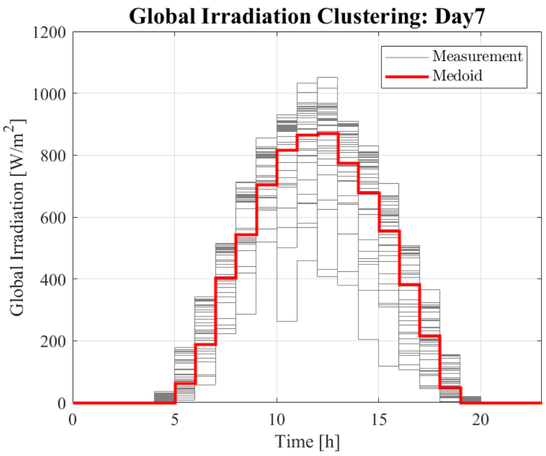


(d) Example irradiation cluster for typical day 7

Figure 5: Outside temperature/global irradiation load curves and example clusters for Rolle in 2016

# 7. Building Energy Systems

The challenge is to propose a computation method providing both the conceptual design and the yearly load scheduling with sufficient precision in a reasonable computing time of a few seconds. The model therefore implements:

- an optimal operation strategy to provide comfort (heating, cooling and electricity) in the buildings using appropriate temperature level;
- hourly time steps to provide sufficient accuracy;
- part-load efficiencies, start-up and shutdown of the equipment;
- centralized and decentralized energy technologies;
- thermal and electrical storage;
- thermal mass of the buildings as heat storage with variable indoor temperature;
- straightforward integration of additional energy sink, source or storage such as power to gas (P2G), gas to power (G2P), residual heat source and energy storage.

The proposed method generate various conceptual design (scenario) of the urban energy system, without going into the detail of the energy network's topology, using process integration and multi-objective optimization techniques. The method is characterized by the use of:

- multi-objective parametric optimization of a MILP formulation for the process integration;
- a two-level decomposition of the problem at building and district scale;
- building energy system (BES) integrated as a meta-model at district scale;
- spatial, temporal and typological data reduction techniques;
- cyclic constraints for thermal and electrical storage;
- piece-wise linearization for efficiencies and distribution temperatures.

The generated alternatives are compared with key performance indicators such as CAPEX and OPEX as a function of the sizes and operation of centralized and decentralized energy conversion equipments.

## 7.1. Data reduction

### Spatial data reduction

Spatial data reduction aims at identifying typical geographical regions with identical climatic conditions The applied approach described in [14] uses the k-medoids technique which provide more robust results than the commonly applied k-means technique [4]. The cluster centers are defined from the initial data set based on the smallest sum of squared distances within each cluster.

The data set include the number of heating (HDD) and cooling (CDD) degree days as well as the annual global horizontal irradiance (GHI) of a reference year (DRY) profile with hourly resolution. The annual cyclicity of the former climatic states supports the assumption of considering the weather data as constant over the entire equipment lifetime, hence decreasing the temporal simulation scope from about $20^{years} \times 8760^{hours}$ to $1^{years} \times 8760^{hours}$ time steps. The definitions of these parameters are expressed in equations (1)-(3) for each observation (i), where the index (d) represents a day and $T^{amb}$ the mean daily ambient temperature.

$$HDD_i = \sum_{d=1}^{365}(18 - T_{i,d}^{amb}) \qquad \forall T_{i,d}^{amb} \leq 15 \tag{1}$$

$$CDD_i = \sum_{d=1}^{365}(T_{i,d}^{amb} - 18) \qquad \forall T_{i,d}^{amb} \geq 18.3 \tag{2}$$

$$GHI_i = \sum_{d=1}^{365}(GHI_{i,d}) \tag{3}$$

To guarantee a reliable representation of the original data by the reduced data space, a minimum acceptable number of clusters are defined on the basis of two quality indicators:

- The error in load duration curve (ELDC) indicating the global standard deviation of the original and clustered load curves;
- The mean profile deviation evaluating the difference between the observations and their representative cluster medoid.

The spatial cluster layout resulting from the application of the method at the communal scale in Switzerland is illustrated in Figure 6.

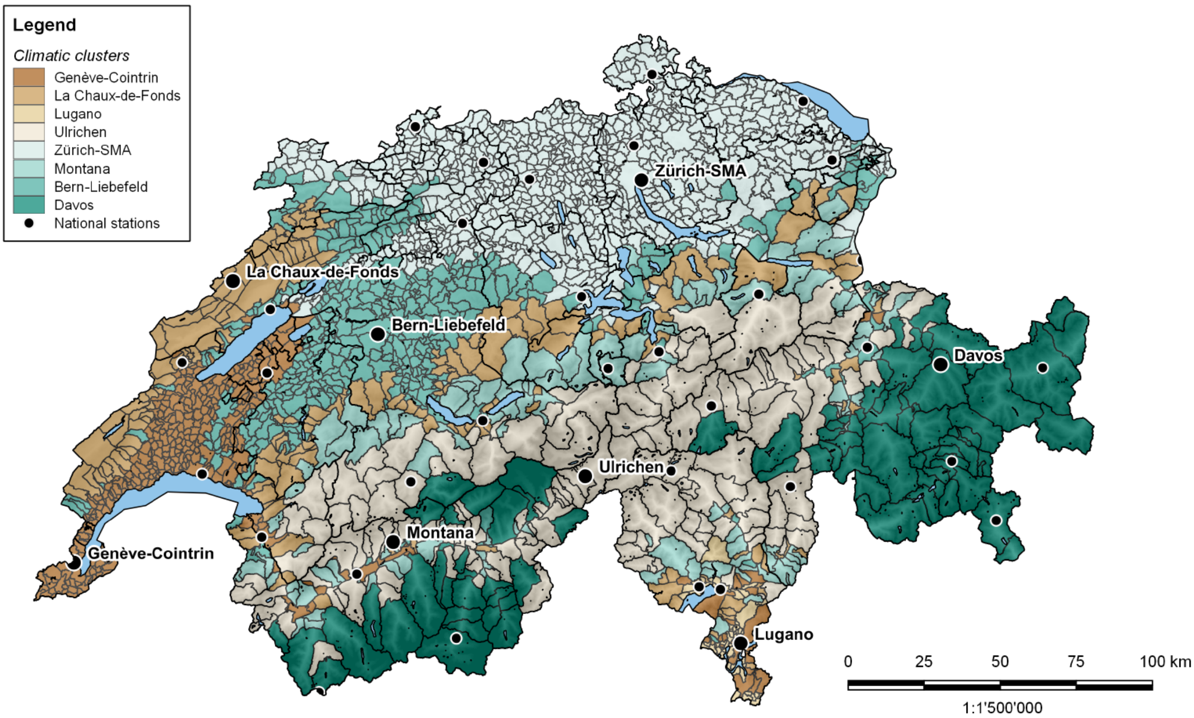


Figure 6: Typical climatic zones in Switzerland [11]

## Temporal data reduction

In addition to the spatial dimension reduction, a second k-medoids clustering method is performed to decrease the temporal input data of the problem from 8760 hours hourly DRY profile to 6 to 12 $\times$ 24 hours typical operating periods with, in addition, 2 extreme periods to reflect peak demand hours. While similar performance indicators have been used to define the best partition number, solely two independent variables have been used: the daily ambient temperature and the global solar irradiance. Further information on the applied approach are given in [9] and [12]. Table 3 provides the selected days and annual frequency of occurrence which allow, as an initial approach, to extract the clustered load curves from the original DRY profiles.

Table 3: Temporal cluster centers and occurrence for each typical climatic zone

| Station | | Indexes | | | | | | | | | | | |
|---|---|---|---|---|---|---|---|---|---|---|---|---|---|
| Geneva-Cointrin | days | 264 | 59 | 222 | 72 | 206 | 7 | 254 | 169 | | | | |
| | freq. | 54 | 46 | 17 | 49 | 52 | 68 | 49 | 30 | | | | |
| Bern-Liebefeld | days | 236 | 209 | 74 | 138 | 336 | 263 | 309 | | | | | |
| | freq. | 53 | 52 | 57 | 52 | 46 | 47 | 58 | | | | | |
| Zürich-SMA | days | 343 | 147 | 74 | 182 | 309 | 122 | 219 | | | | | |
| | freq. | 59 | 35 | 37 | 47 | 77 | 52 | 58 | | | | | |
| Davos | days | 223 | 198 | 264 | 105 | 275 | 250 | 336 | 64 | 331 | 125 | 236 | 55 |
| | freq. | 31 | 40 | 43 | 37 | 38 | 28 | 36 | 11 | 36 | 9 | 14 | 42 |
| Lugano | days | 74 | 137 | 364 | 95 | 325 | 209 | 227 | 224 | | | | |
| | freq. | 54 | 48 | 64 | 42 | 57 | 36 | 48 | 16 | | | | |
| Disentis | days | 349 | 123 | 74 | 228 | 278 | 242 | 17 | | | | | |
| | freq. | 59 | 57 | 49 | 52 | 57 | 37 | 54 | | | | | |
| Piotta | days | 233 | 242 | 214 | 287 | 61 | 182 | 97 | 8 | 78 | 33 | 260 | |
| | freq. | 33 | 23 | 16 | 28 | 29 | 22 | 35 | 49 | 38 | 65 | 27 | |

## Typological data reduction

A further spatio-temporal classification step can be performed at the building level. A district might indeed be expressed as a collection of typical service demand profiles with a given probability of occurrence. Therefore, the temporal data reduction method is applied by considering 8 specific demand profiles for each urban area:

(i) annual uncontrollable electricity;

(ii) domestic hot water;

(iii) internal heat loads;

(iv) available solar potential;

(v) space heating and

(vi) space cooling energy signature;

(vii) diurnal and

(viii) nocturnal utilization hours.

This classification into a reduced set of typical energy profiles foe buildings allows to reduce the number of profile by four with errors less than 10% [13], which remains within an acceptable range of tolerance.

## 7.2. Building energy system (BES) model

The modeling framework relies on MILP techniques to describe both the continuous (e.g. output modulation) and logical (e.g. start-up) behavior of the devices. An overview of the latter is illustrated in Figure 7; it comprises an air-water heat pump as well as electric auxiliary heaters to satisfy the different heating requirements. Energy is stored in either stationary batteries, the domestic hot water and buffer tanks or the building envelope. Photovoltaic and solar collector panels act as renewable energy sources, the latter being only connected to the domestic hot water tank in regard to the strong seasonal disparity of generation potential and space heating demand. The different energy systems are finally interconnected through the main energy distribution networks: the natural gas, electricity and fresh water grid. Although the figure solely illustrates an air–water heat pump as primary thermal conversion unit, a cogeneration heat plant (CHP) device or a combination of multiple technologies might also be selected by the solver. To propose future, efficient energy systems to the different stakeholders, solely solid oxide (SOFC), and low temperature proton exchange membrane fuel cells (LPEM) are considered as CHP units in the following structure. In addition, it is worth noting that the final hydraulic layout (including, e.g., pumps, by-passes, three-way valves) of the designed BES may be implemented differently, according to the selected solution. Further details on the optimization problem formulation and input data are reported in [11].

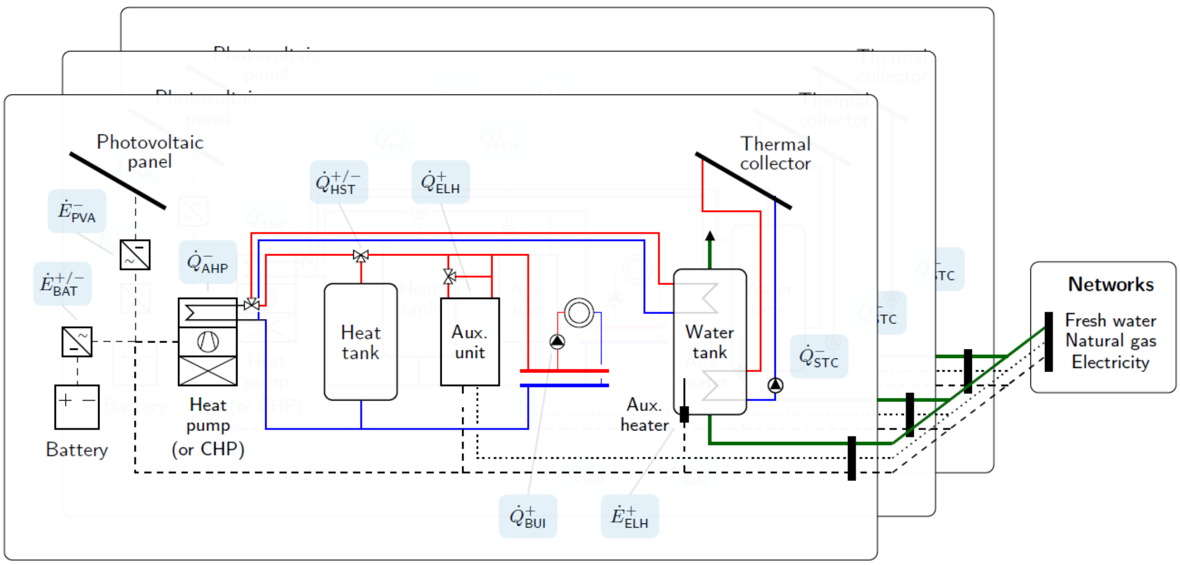


Figure 7: Building energy system structure and the respective control variables (blue) [2]

### Sets

The sets and their respective indices used in the MILP formulation are reported in Table 4.

Figure 8 illustrates the building energy system structure. Hydraulic connections, valves and circulation pumps are not considered in the model.

Table 4: List of defined sets with description

| Set | Index | Increment | Cyclic | Description |
|---|---|---|---|---|
| P | p | dp | No | Period (day) |
| T | t | dt | Yes | Time (hour) |
| K | k | | No | Temperature level |
| U | u | | | Utility types |
| B | b | | | Building |

### Model input and output

The different domestic service demands of each dwelling have been estimated using both statistical and normalized data. Indeed, considering the approach developed by [6], space heating demands are determined through the means of the energy signature denition while the remaining service requirements (domestic hot water preparation and electricity) are evaluated using standards of the Swiss society of engineers and architects (SIA 2024 [10]). The minimal set of data recquired for the systematic generation of alternative scenario of building energy system are reported in Table 5

Subsequently to the size and operation profile of the equipments, specic key performance indicators are evaluated to highlight the integration of renewable energy sources within the considered district. Within this context, both the self-suciency (SS) and self-consumption (SC) are implemented [7]. While the former reflects the share of generated electricity consumed on-site, the latter expresses the share of generated electricity consumed on-site in regard to the total demand.

Table 5: Input data for the systematic generation of alternative scenario at building scale

| Field | Description | Unit |
|---|---|---|
| Objective and Limits | Objective Function (OPEX, CAPEX) | - |
| | Upper limit for the specific annualized investment | $CHF/m^2 \cdot y$ |
| Time data | Typical operating days number (1-365) | - |
| | Frequency of the typical days | d/y |
| | Extreme operating periods | - |
| Electrical profiles | Uncontrollable load profiles | kW |
| Building data | Grid parameter, transformer/house connection | - |
| | Share of useful roof | - |
| | Solar gain (fraction of house area) | - |
| | Reference indoor temperature | $^{\circ}C$ |
| | Specific heat transfer coefficient of the building | $kW/K \cdot m^2$ |
| | Type and period of construction/renovation | - |
| | Specific electric needs | $W/m^2$ |
| | Reference Energetic Area or heated surface | $m2$ |
| | Sizing return temperature of the heating system | $^{\circ}C$ |
| | Sizing supply temperature of the heating system | $^{\circ}C$ |
| | Number of inhabitant | cap |
| | Specific domestic hot water demand | $W/m^2$ |
| | Building type | - |
| | Unique identifier | - |
| | Number of floors of building | - |
| | Specific heat capacity of the building | $Wh/K \cdot m^2$ |
| Technologies | Possible presence of equipments in building | [0, 1] |

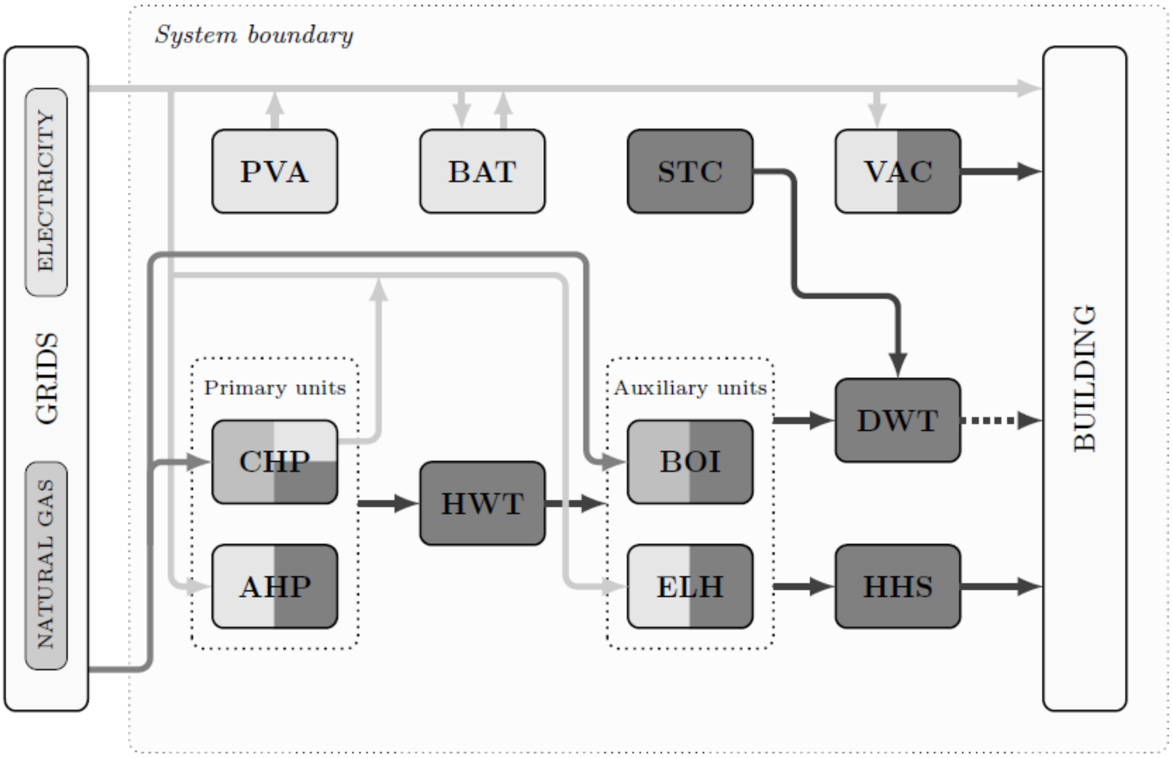


Figure 8: Energy system structure: electricity flows (light grey), natural gas flows (grey), heating/cooling flows (dark grey) [14]

## 7.3. Formulation of the multi-objective optimization model

The optimal integration of the building energy technologies is formulated as a multi-objective optimization problem based on a MILP formulation with the annual building operating expenses (OPEX) as the main objective. The OPEX comprise both the natural gas and power grid exchanges. The former are defined in equation (4) where ($op$) refers to the grid energy tariffs, ($E$) to the electrical power flows, ($H$) to the chemical–natural gas–power flows, (d) to the indexed time step duration, and ($\Sigma$) to the set of decision variables reported in [11].

$$\min_{\Sigma} \sum_{p=1}^{P} \sum_{t=1}^{T} \left( \dot{Q}^{+}_{grid,p,t} \cdot op^{th,+}_{p,t} + \dot{E}^{+}_{grid,p,t} + \cdot op^{el,+}_{p,t} - \dot{E}^{-}_{grid,p,t} \cdot op^{el,-}_{p,t} + \dot{H}^{+}_{grid,p,t} \cdot op^{ng,+}_{p,t} \right) \cdot d_p \cdot d_t \quad (4)$$

The second objective, formulated as a parametric $\epsilon$-constraint in the optimization problem, is the present capital expenses related to the different unit purchases over the project horizon ($N$). In equation (4), ($I_{1,u}$) and ($I_{2,u}$) denote the linear cost function parameters, ($y_u$) the unit existence while ($f_u$) is the device sizing variable. In addition, ($N_u$) refers to the unit lifetime, ($r$) the project interest rate and ($rep_u$) to the number of unit replacements over the project horizon.

$$\sum_{u=1}^{U} (I_{1,u} \cdot y_u + I_{2,u} \cdot f_u) + \sum_{u=1}^{U} \sum_{n=1}^{rep_{u,N}} \frac{1}{(1+r)^{n \cdot N_u}} \cdot (I_{1,u} \cdot y_u + I_{2,u} \cdot f_u) \leq \epsilon_I \quad (5)$$

Finally, a third objective function implemented as an $epsilon$-constraint is used to represent the power network constraint: the grid multiple (GM). As detailed in equation (6), this parameter limits the building power profile peaks ($\dot{E}_{grid}$) with respect to the daily average demand and thus decreases the consequent stress on the distribution network from strong demand/supply surges. For the sake of readability, the total period duration is denoted by ($n_t$).

$$\frac{\left(\dot{E}^{+}_{grid,p,t} - \dot{E}^{-}_{grid,p,t}\right)}{\frac{1}{n_t}\sum_{t=1}^{T}\left(\dot{E}^{+}_{grid,p,t} - \dot{E}^{-}_{grid,p,t}\right)} \leq \epsilon_{GM} \tag{6}$$

### Heat Cascade

The heat cascade balances the system heat loads while satisfy the second law of thermodynamics. Equation (7) thus defines the thermal energy balance of each temperature interval k where ($Q^{-}_{u_h,k}$) represents the released heat of utility ($u_h$), ($Q^{+}_{u_c,k}$) represents the heat demand of utility ($u_c$), and ($R_k$) the residual heat cascaded to next interval (k+1). In addition, no heat is cascaded at the first and last intervals to ensure a closed thermal energy balance.

$$\begin{aligned} \dot{R}_{k,p,t} - \dot{R}_{k+1,p,t} &= \sum_{u_h=1}^{U} \dot{Q}^{-}_{u_h,k,p,t} - \sum_{u_c=1}^{U} \dot{Q}^{+}_{u_c,k,p,t} \\ \dot{R}_{1,p,t} &= \dot{R}_{n_k+1,p,t} \qquad \forall p \in \mathsf{P},\ t \in \mathsf{T},\ k \in \mathsf{K} \end{aligned} \tag{7}$$

### Energy Balances

The electrical and natural gas energy balances are defined in equation (8) where ($E^{-}_{build}$) refers to the building uncontrollable load profile.

$$\begin{aligned} \dot{E}^{+}_{grid,p,t} + \sum_{u=1}^{U} \dot{E}^{+}_{u,p,t} &= \dot{E}^{-}_{grid,p,t} + \sum_{u=1}^{U} \dot{E}^{-}_{u,p,t} + \dot{E}^{-}_{b,p,t} \\ \dot{H}^{+}_{grid,p,t} &= \sum_{u=1}^{U} \dot{H}^{-}_{u,p,t} \qquad \forall p \in \mathsf{P},\ t \in \mathsf{T} \end{aligned} \tag{8}$$

### Cyclic Conditions

To prevent any energy accumulation between the different independent operating periods ($p$), cyclic constraints of equation (9) enforce all system states to return to their initial value at the end of each control horizon ($n_t$). The latter constraints target the dwelling temperature ($T_b$) as well as the thermal ($Q$) and electrical energy ($E$) stored in the respective storage units. The typical days ($p$) represent indeed different operating conditions with a given probability of occurrence during the system lifetime.

Equation (9) is therefore included in the problem formulation to avoid any energy bias.

$$\begin{aligned} T_{b,p,1} &= T_{b,p,n_t} \\ Q_{u,p,1} &= Q_{u,p,n_t} \\ E_{u,p,1} &= E_{u,p,n_t} \qquad \forall p \in \mathsf{P},\ u \in \mathsf{U} \end{aligned} \tag{9}$$

## Unit Sizes

The unit existence ($y_u$) and logical state on/off ($y_{u,p,t}$) are expressed in equation (9) where ($F_u^{min}$) and ($F_u^{max}$) describe the device minimal and maximal sizing values.

$$\begin{aligned} y_u \cdot F_u^{min} \leq f_u \leq y_u \cdot F_u^{max} \\ y_{u,p,t} \leq y_u \qquad \forall u \in \mathsf{U} \end{aligned} \tag{10}$$

# 8. Single Building Multi-Energy Systems Optimization

To explore possible bottleneck problems of the electrical grid, it is necessary to obtain a variation of possible operating points and energy scenarios. Therefore, the energy systems of single buildings are investigated on a first stage. On a second stage the multi-objective optimization is carried out on every building within the selected area.

## 8.1. Solutions on Single Building Level

The methodology from Section 7 gives the building model. The data reduction is preformed according to the meteorological area of Rolle (see Figure 5).
A multi-objective optimization is performed considering capital expenses (CAPEX) and operating expenses (OPEX) both per Reference Energetic Area (or heated surface see Table 5).
The main objective is the minimization of the OPEX (see Equation (4)). CAPEX is constrained according to Equation (5).
Figure 9 shows the Pareto curve for an exemplary building for LV transformer HÔPITAL-TR3716.

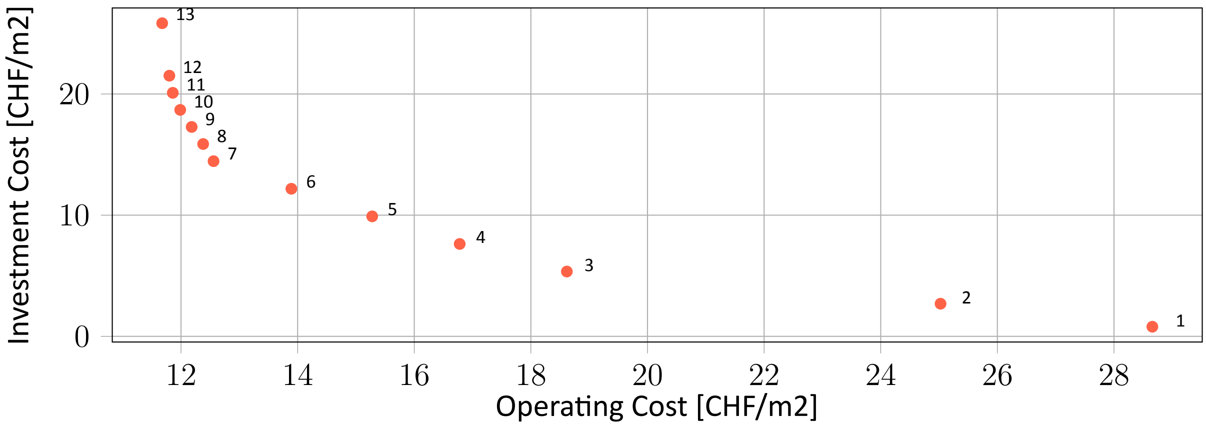


Figure 9: Pareto curve of a single building for LV transformer HÔPITAL-TR3716. Minimization of OPEX while constrained CAPEX and related to the Reference Energetic Area (per m2)

The Pareto Points in Figure 9 arrange in clearly distinguishable groups: Solution 13 and 1 are the upper and lower bound of the interval of feasible CAPEX constraints. The unconstrained OPEX minimization gives Scenario 13 with the highest CAPEX. In contrast, the result of a CAPEX minimization is the lowest possible CAPEX constraint in Solution 1. Solution 2 seems to form its own group between the lower bound (Scenario 1) and a group containing Solution 3 to 7. This leaves Scenario 8-12 forming a group. Different technologies are responsible for this particular formation of subgroups within the Pareto curve. Figure 10 displays the detailed association of the configuration of the energy system to each solution.

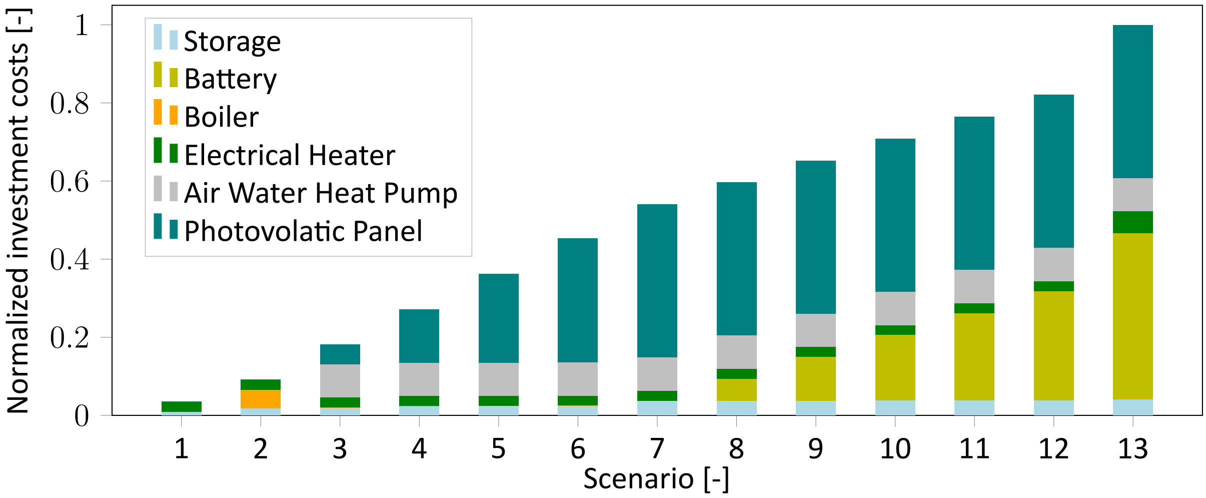


Figure 10: Technology details of the detected Pareto points (see Figure 9. Pareto point 1 is referring to Scenario 1. The investment costs are normalized to the maximum CAPEX (Scenario 13).

Low investment costs correspond to gas based energy systems. With respect to the unrealistic boundaries, Scenario 2 is the only gas based solution. Lowering the operating expenses by allowing to increase capital expenses leads to an electricity based energy system with air water heat pump and solar panels. Within this group (Scenario 3-7) the number of installed panels is increasing until the roof potential is fully exploited. Decreasing the operating costs further leads to the installation of Batteries (Scenario 8-12). However, the operating costs are not reduced significantly whereas the capital expenses are rapidly increasing (see Figure 9).

## 8.2. Solution on Single Building Level with Grid Multiple Constraint

To lower the stress on the network, it is possible to introduce the Grid Multiple Parameter (GM) (see Equation 6). This Parameter constraints the height of the peak with respect to the average per day. For example GM $= 2$ would lead to a peak which has to be lower than twice the daily average. The feasible lower bound of the Grid Multiple is GM$= 1$, which leads to a constant electric demand profile. Figure 11 shows the Pareto curve of a single building with different Grid Multiple. Figure 12 shows the technology detail of each Pareto point for GM $= 2$ in comparison to the unconstrained grid profile.

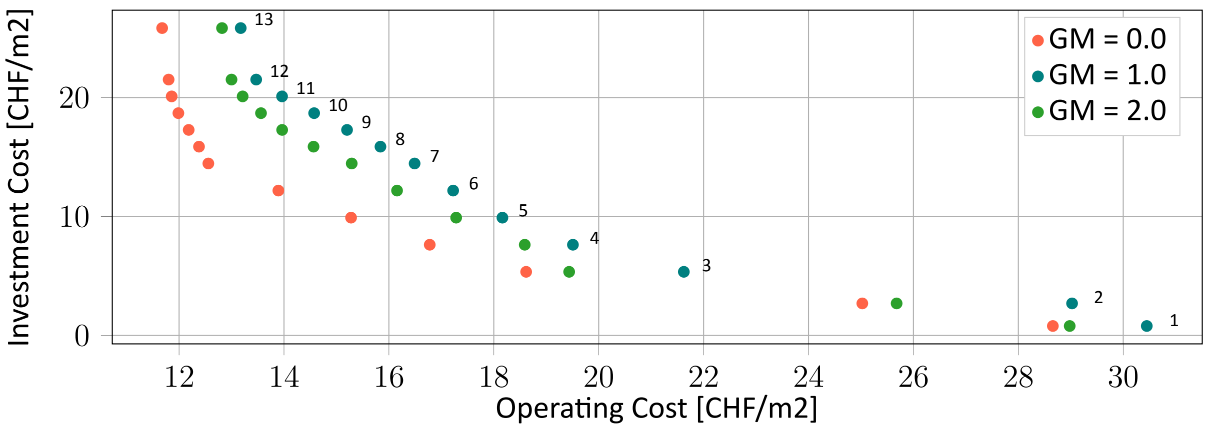


Figure 11: Pareto curve of a single building for LV transformer HÔPITAL-TR3716 with different Grid Multiple (GM) constraints. Minimization of OPEX while constrained CAPEX, both related to the Reference Energetic Area (per m2). GM $= 0$ is the solution without Grid Multiple (compare with Figure 9).

To lower the stress on the network, the model reacts in two ways. On the one hand it is installing batteries in earlier scenarios, on the other hand reducing the amount of photovoltaic panels. Both effects lead to higher operation costs, losses come along with the battery and higher electricity costs with less photovoltaic panels.

## 8.3. Solution on District Level

The multi-objective optimization with different CAPEX constraints is done for every building, which is connected to the LV transformer. The optimization is performed for every building separately, the district scenario however is aggregated by building scenario. For a better overview about the buildings in the district, the district solution is displayed by average and discussed in the following. Thereby, the average of an attribute $a_i$ (for example CAPEX or OPEX) is divided by the sum of the Reference Energetic Area ERA within the district (see Equation 11).

$$A_{average} = \frac{\sum_{i=1}^{n_b} a_i}{\sum_{i=1}^{n_b} ERA_i} \tag{11}$$

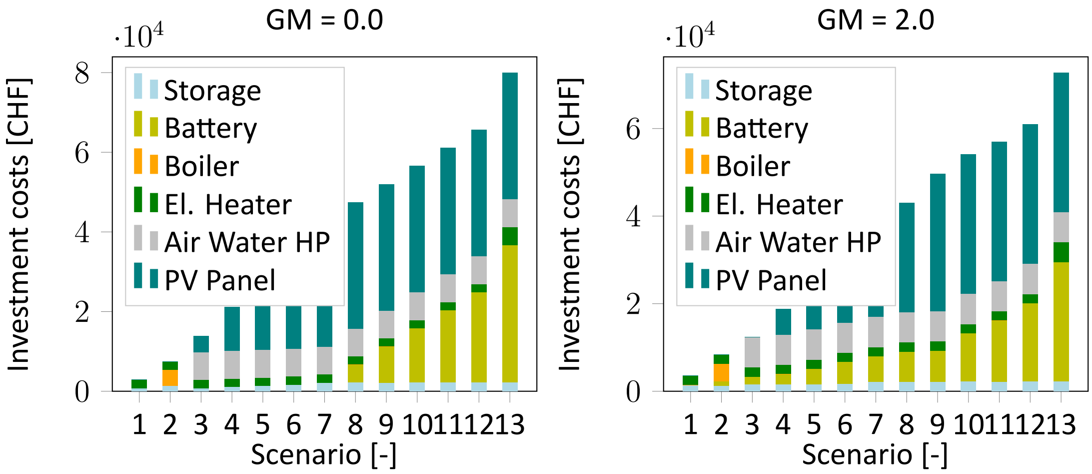


(a) Unconstrained grid profile.

(b) Grid multiple GM $= 2.0$.

Figure 12: Technology details of the detected Pareto curves (see Figure 11). Pareto point 1 is referring to Scenario 1.

Figure 13 compares the Pareto curve of one building with the average Pareto curve of the district. The exemplary building is higher in investment cost but lower in operating costs. However, the shape of the Pareto curves is the same. This leads to the conclusion, the energy system of each building in the district is similar within each scenario.

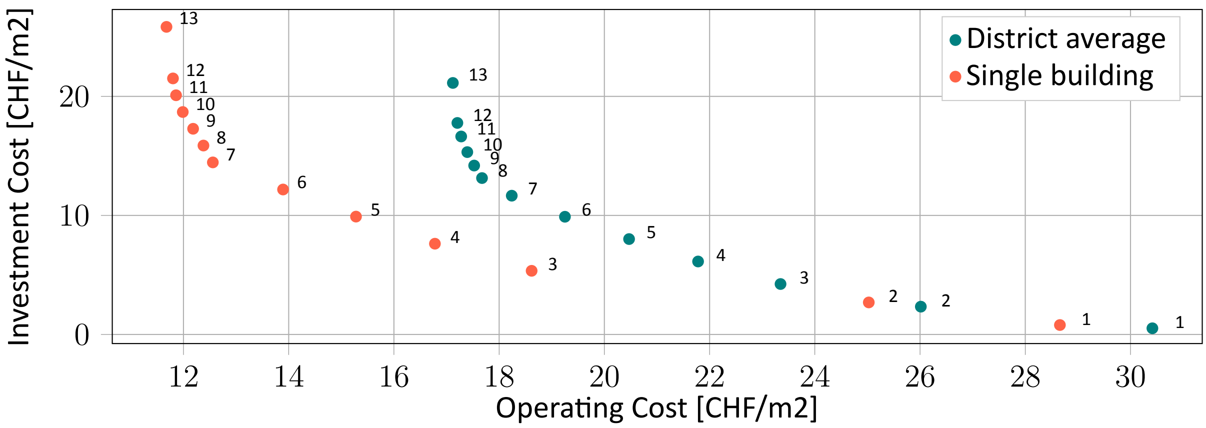


Figure 13: Pareto curve of a single building for LV transformer HÔPITAL-TR3716 in comparison with the average of the whole district.

Figure 14 displays the details of the energy system within each scenario. The configuration is similar between the district and the single building (see Figure 10). However, Scenario 2 shows heterogeneous energy systems within the district. There is a restriction in the model, which prevents to install boiler and heat pump at the same time. Where Scenario 2 of the single building was purely natural gas based, some buildings within the district are electricity based with photovoltaic panels and an air water heat pump.

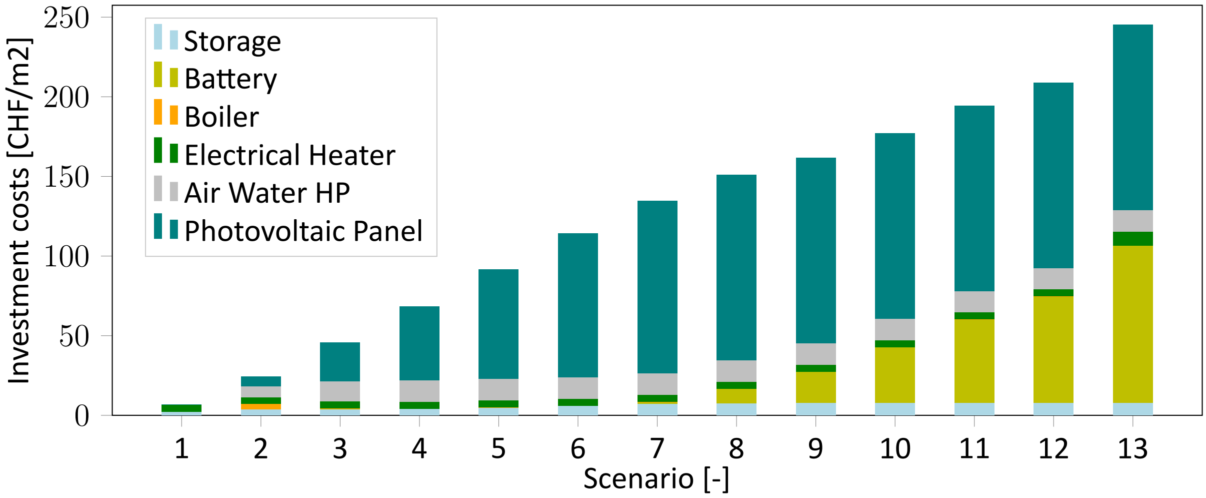


Figure 14: Technology details of the aggregated Pareto points from the district (see Figure 13. Pareto point 1 is referring to Scenario 1.

The investigation of the grid multiple parameter shows that especially photovoltaic panels and batteries have an impact on the electric network. Figure 15 shows their evolution within district at the different scenarios. The battery is installed during scenarios with higher CAPEX - constraints, when the potential of the roofs is exploited (scenario 8). At scenario 3 20% of the available area is used in the district.

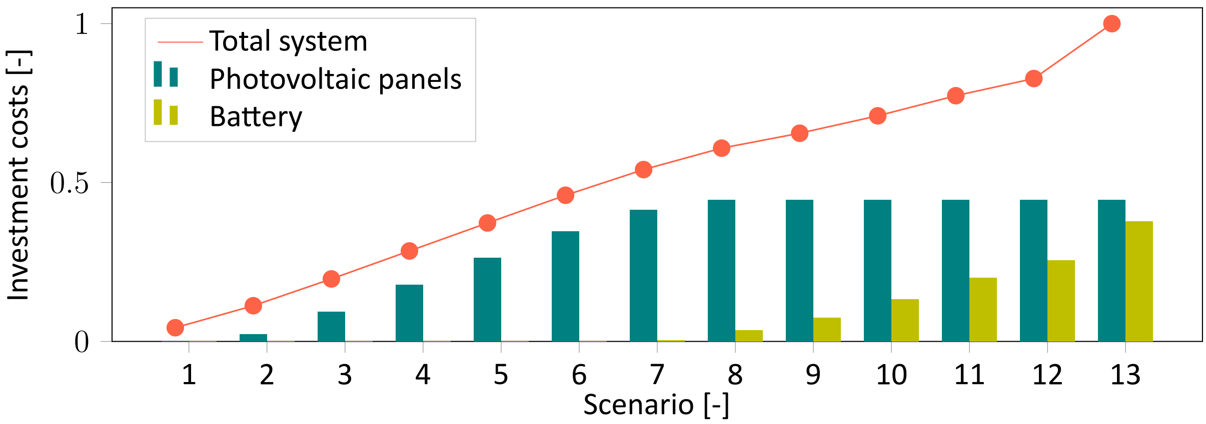


Figure 15: Evolution of PV and Battery installation with in the Pareto curve. Pareto point 1 (see figure 9) is referring to Scenario 1.

# 9. Grid Modeling and Impact

The result of the multi-energy optimization gives for each building, each typical day given by the temporal clustering and each scenario given by the pareto front the electrical grid exchange. However, this optimization doesn't for now take into account the grid constraints as the transformer loading, the maximum voltage deviation, the line ampacity, the frequency deviation or harmonics. Thus, the aim of the section is to analyze whenever the optimization result is feasible or not from the electrical grid perspective.

To answer this question, the low voltage grid HOPITAL-TR3716 has been modeled using OpenDSS power flow solver. Since each building is not individually connected to grid, their grid exchange have been aggregated at the injection points, shown as red points in figure 16. In the frame of this simple analysis, a scenario will be considered as feasible if it doesn't lead to any transformer overloading and any voltage deviation higher to 3% (DACHCZ [2]).

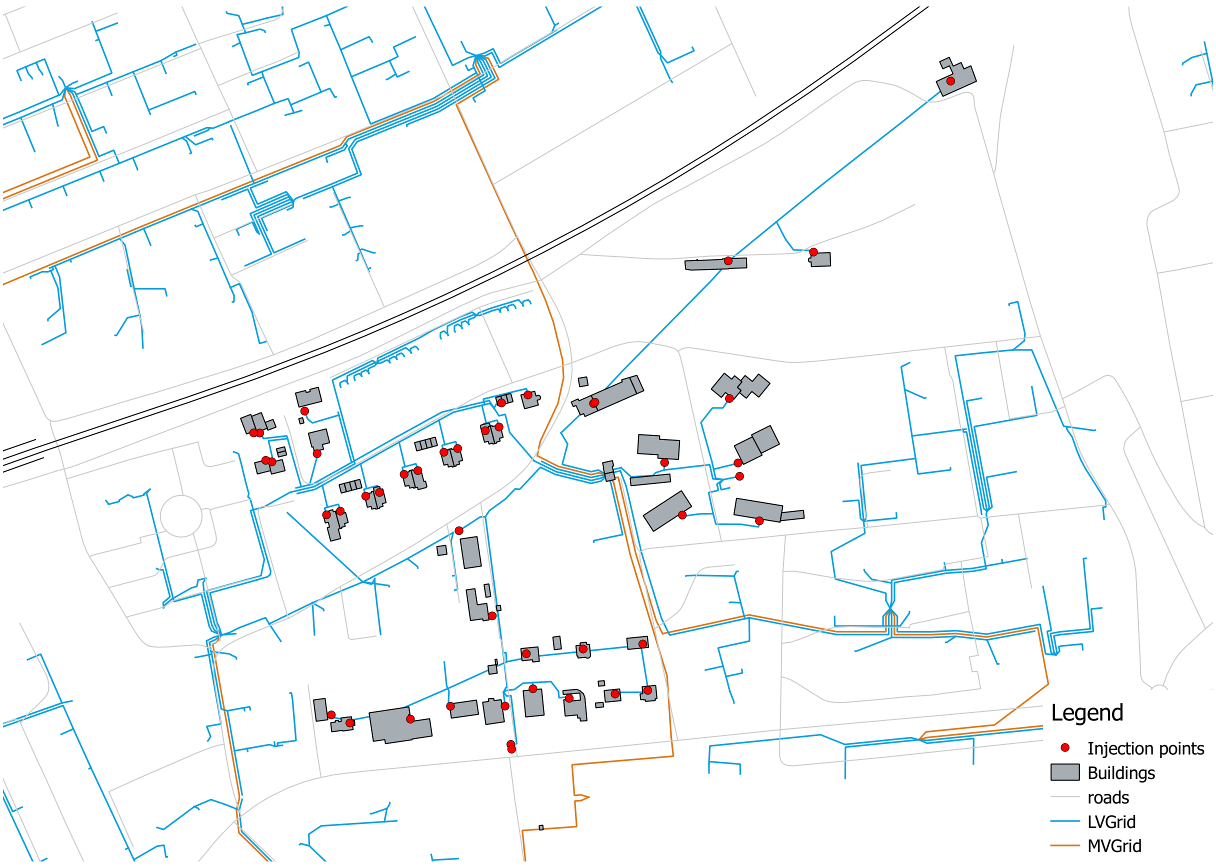


Figure 16: GIS diagram of the low voltage (blue) and medium voltage (orange) grids as well as the buildings connected to the low voltage grid HOPITAL-TR3716 and their injection points.

As shown in figure 14 the investment cost for PV modules increases with the scenario number due to the increasing CAPEX limit. Since scenario 2 roughly corresponds to current mix in Switzerland and scenario 3 to the objective of the Swiss energy strategy for 2050 in terms of PV share, this prompts us to compare these 2 cases.

The real power flow at the low to medium voltage transformer is shown is figure 17, for each typical day and both scenario 2 and 3. One can observe that every day has 3 distinct peaks, one in the morning, one around noon and one in the evening. This is the consequence of using standard load profiles (SIA) with a one hour resolution as input of the multi-energy optimization. Since each building use one of the 8 available SIA profile, among the 73 buildings present in this low voltage grid, many use the same profile resulting in synchronized peaks at the transformer level. These load profiles will soon be replaced by load profiles generated with allocation based model that distribute unique load profile for each building.

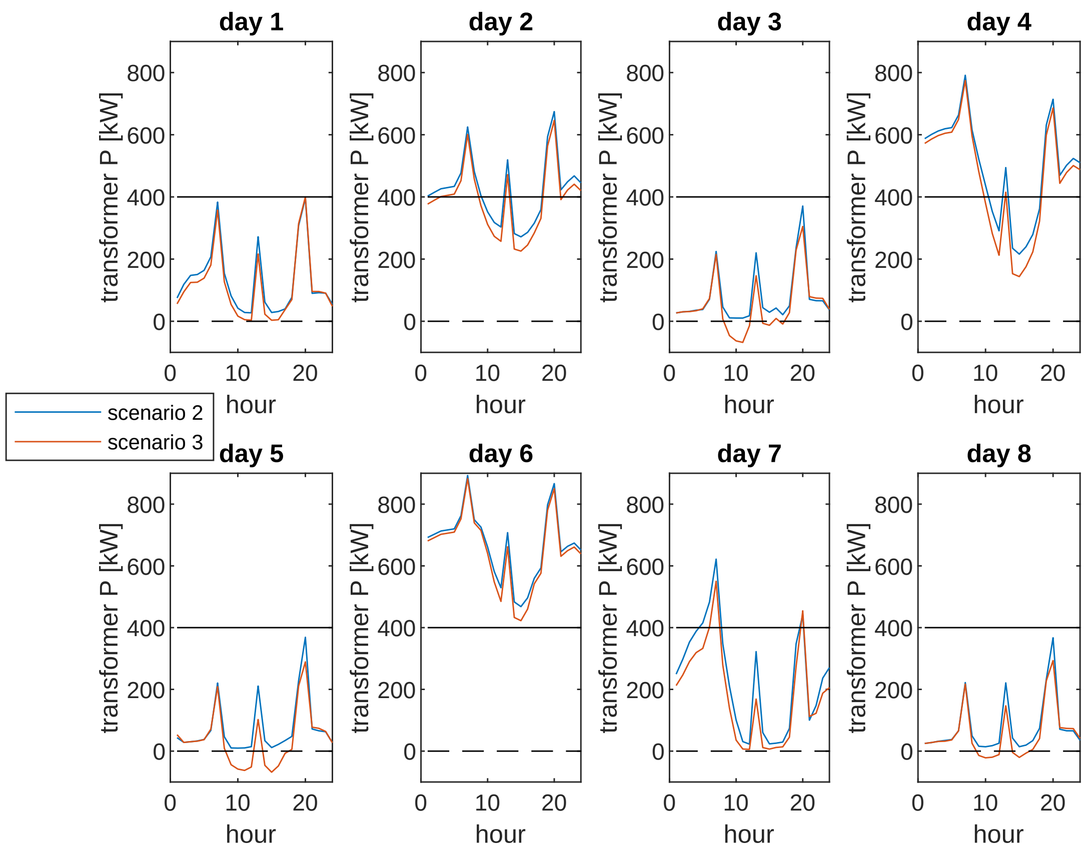


Figure 17: Real power flow at the transformer level for each typical days and both scenario 2 and 3. A positive value represents a flow from the medium to low voltage grid.

Four of the eight typical days show a power flow at the transformer higher than its nominal power 400 kW. Since scenario 2 represents the current mix in Switzerland, the only possible conclusion is that either there is less electric heating in this low voltage grid compared to the current mix or the SIA load profiles overestimate the real electrical load profile as already remarked in the report [16]. The power flow resulting from scenario 3 is generally below scenario 2 due to a higher PV capacity as shown in figure 14. A negative power flow even appears in days 3, 6 and 8 however way below the transformer capacity.

The loads for both scenarios are above the transformer capacity during the whole day number 6. This typical day corresponds to the seventh day of the year according to table 3 explaining the high demand for electric heating. Such a high load would lead a voltage deviation up to 11% as shown in figure 18.

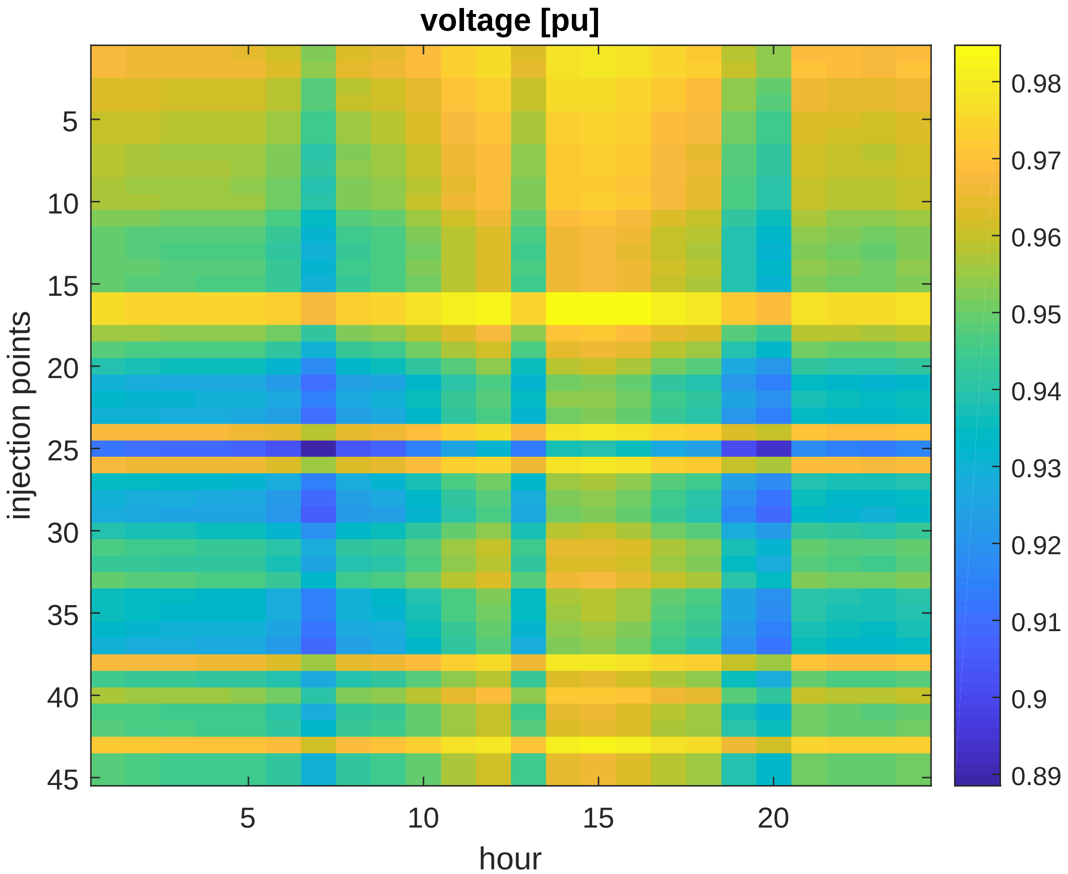


Figure 18: Normalized voltage for each injection point and each hour of the typical day 6, scenario 2.

Then the voltage constraint violation can be localised in the low voltage grid. For example at 7am, figure 19 shows that the voltage deviation is stronger in the south part of the low voltage grid.

Scenario 2 and 3 analyzed until here don't include any storage with battery. To study the impact of the storage on the electrical grid, scenario 7 that has high PV capacity but no battery will be compared to scenario 13 in which investment in storage is very high. Figure 20 shows that a few peaks of the power flow at the transformer level are curtailed with the storage. However since the storage control is based on a cost minimization for the building, it doesn't always decrease the daily peaks. Many solutions exist to minimize these peaks, for example the use of the grid multiplier constraint define is section 7.3 or by adding a power based tariff in the operation costs.

During day 3 for both scenario 7 and 13, the high PV capacity leads to an reverse power flow higher than the nominal transformer capacity. It also leads to an overvoltage for most of injection points as

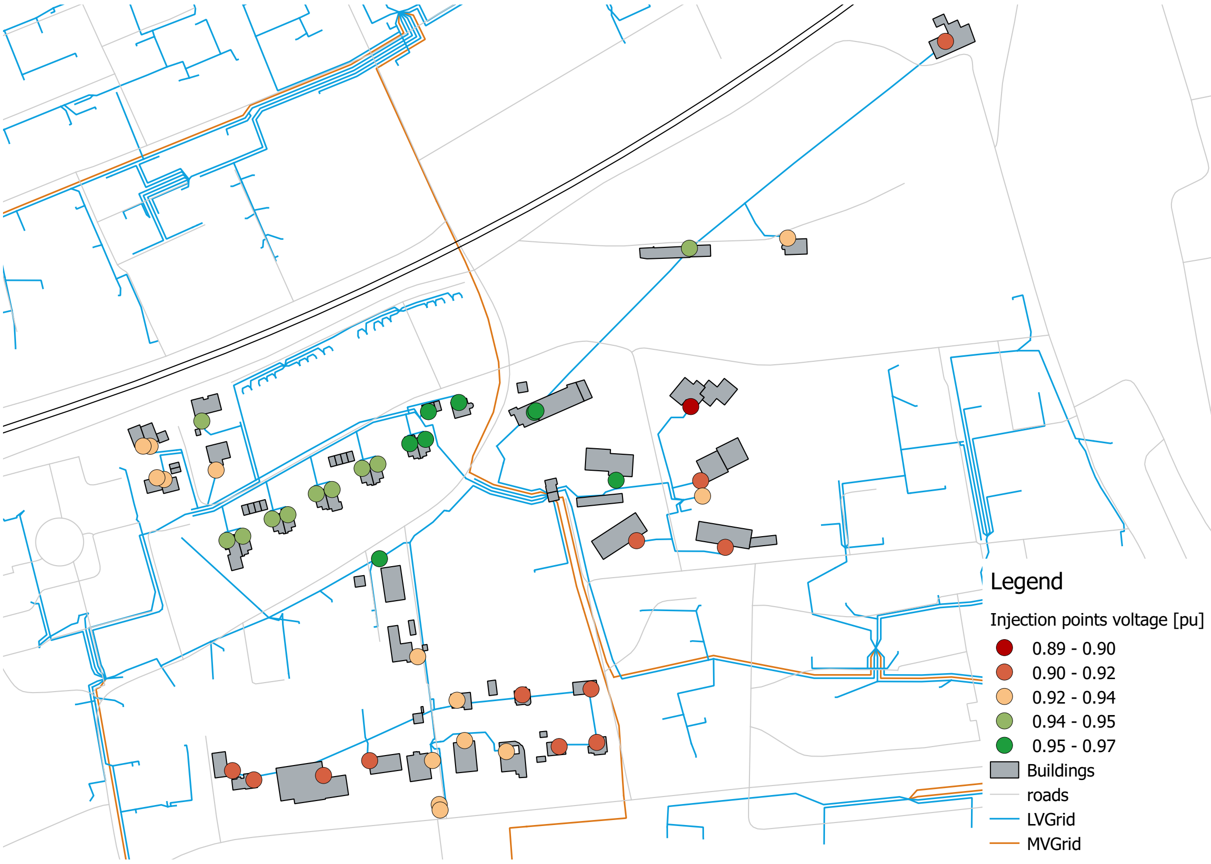


Figure 19: Voltage deviation at each injection point for the scenario 2, typical day 6 and at 7am

shown in figure 20.

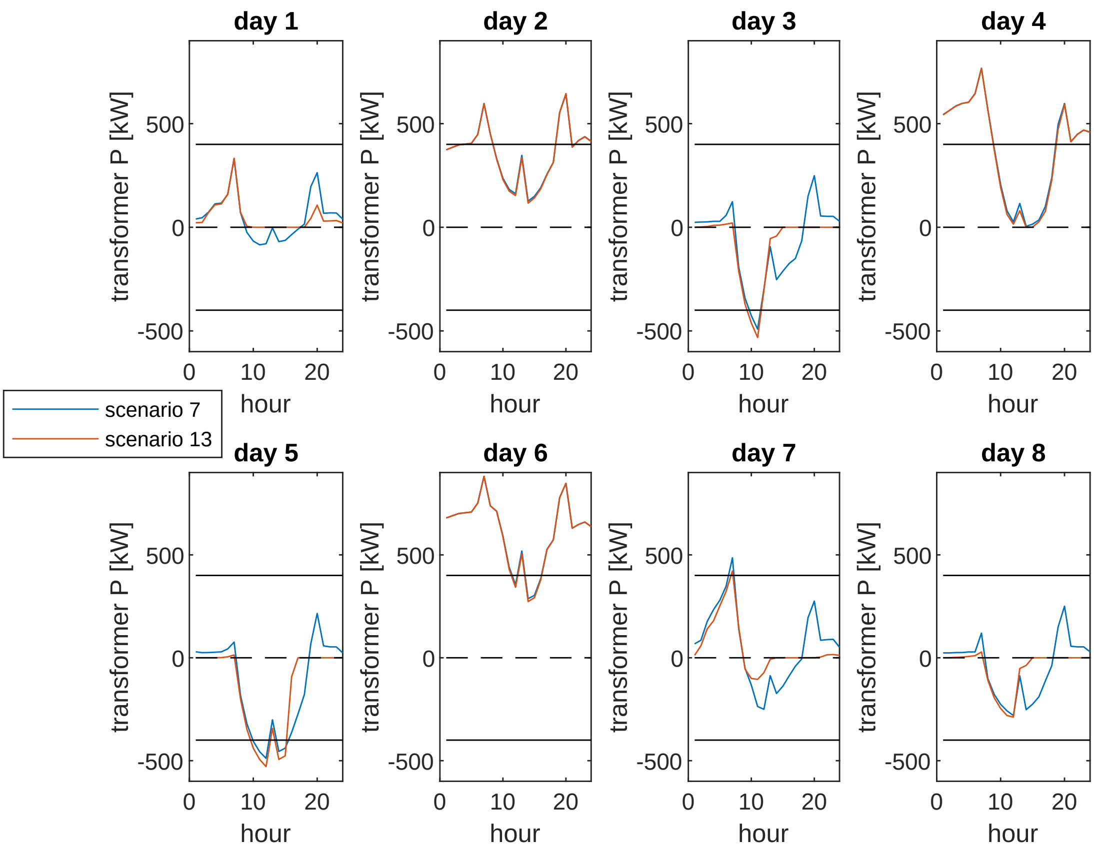


Figure 20: Real power flow at the transformer level for each typical days and both scenario 7 and 13. A positive value represents a flow from the medium to low voltage grid.

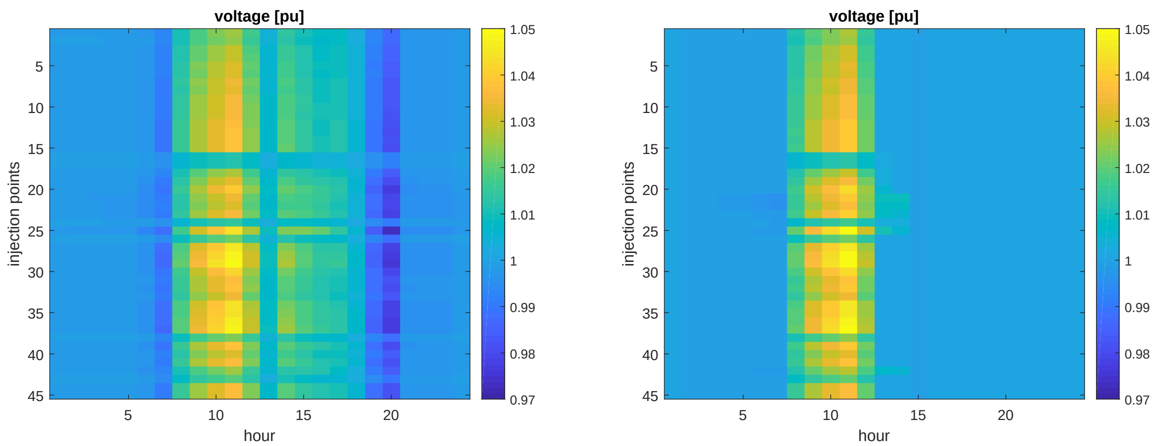


(a) Scenario 7, day 3

(b) Scenario 13, day 3

Figure 21: Normalized voltage for each injection point and each hour

In this section the grid impact measured as the transformer loading and voltage deviation at the injection points has been analysed for a few scenarios resulting of the multi-energy optimization. However the use of standard SIA load profiles which don't have the inherent variability of real load profiles, doesn't allow to evaluate properly if a scenario is feasible or not. The recent measurements from Depsys at the low to medium voltage transformer will be used to build an allocation based model to generate the load profiles. Each load profile will be unique, depend on the electricity consumption for heating and match the building affectation and annual electricity consumption given by the Romande Energie. Moreover the aggregated profiles should match the Depsys's measurements.

# 10. Conclusion and Future Work

The increasing use of renewable energy is a deep going trend mainly supported by the sustained annual growth rate of solar photovoltaic, wind power and biogases. In this context, decentralized power generation and heat pumps technologies are expected to play an increasing role. This evolution is inevitably going to increase the stress on both electricity and gas distribution networks while pushing the development of district heating and cooling (DHC) networks. At the grid level, the inherent uncertainty in renewable energy generation, the trend towards decentralisation and the emergence of new energy prosumers are going to increase bi-directional energy interconnections, therefore challenging the energy networks to balance supply and demand.
The expansion and evolution of the distribution grids is therefore a key issue to ensure a secure and sustainable supply of electricity in the future. Aside from heavily investing in grid reinforcement and additional storage capacities, model predictive control methods provide an interesting option to shift controllable loads toward production periods.

This report presents an integrated approach for the elaboration of alternative scenarios for the future grid evolution. The proposed method allows to optimally design and schedule building energy systems within the context of smart grids. It combines geographical information system, process integration techniques and power flow analysis to model the holistic district energy system including heat cascading and network constraints to ensure power quality. The scenarios at district scale results form the aggregation of optimal energy technology configurations at building scale given as a function of the investment capacity. This approach therefore allows to evaluate the effect of the increase of prosumer capacities in the grid.

In order to limit the computational effort related to presented problem formulation, the time dependent input profiles are clustered into typical operating periods using a k-medoids classification method, hence reducing the problem size from $20^{\text{years}} \times 8760^{\text{hours}}$ to $8 \times 24^{\text{hours}}$. A further classification into a reduced set of typical building's energy profiles allows to reduce the number of profiles even more.

This preliminary implementation of the proposed framework in a district in Rolle allowed highlighting the key elements required to move from a normative analysis towards practical application (Table 6).

Table 6: Further improvements towards practical applications

| Level | Further improvements |
|---|---|
| Model and data | Identify extreme grid operating condition<br>Integrate solar roof/orientation dataset<br>Integrate solar potential on façade<br>Use real electric profiles instead of standard SIA profiles |
| Optimization at building scale | Implement a retroaction loop from power flow analysis<br>Implement battery charge/discharge cycle constraint<br>Consider grid constraints (spotload or linear grid model)<br>Integrate volume constraint for technical room and equipment<br>Consider load profile in temporal clustering<br>Increase time resolution |
| Optimization at district scale | Perform investment scheduling<br>Integrate spatial constraint<br>Consider a Wider range of indicators |

# References


[1] Araz Ashouri. Simultaneous design and control of energy systems. PhD thesis, 2014.

[2] Gerhard Bartak, Hansjörg Holenstein, and Jan Meyer. Technical rules for the assessment of network disturbances. VEO Austria, VSE Switzerland, CSRES Czech Republic, VDN Germany,, 2007. 00007.

[3] European Comission. Eurostat, October 2017.

[4] Samira Fazlollahi, Stephane Laurent, Bungener, Pierre Mandel, Gwenaelle Becker, and François Maréchal. Multi-objectives, multi-period optimization of district energy systems: I. Selection of typical operating periods. Computers & Chemical Engineering, 65:54–66, 2014.

[5] Bundesamt für Energie BFE. Schweizerische Gesamtenergiestatistik 2015. Technical report, Swiss Federal Energy Office, Switzerland, 2015.

[6] Luc Girardin, Francois Marechal, Matthias Dubuis, Nicole Calame-Darbellay, and Daniel Favrat. Energis: A geographical information based system for the evaluation of integrated energy conversion systems in urban areas. Energy, 35:830–840, 2010.

[7] Rasmus Luthander, Joakim Widèn, Daniel Nilsson, and Jenny Palm. Photovoltaic self-consumption in buildings : A review. Applied Energy, 142:80–94, 2015.

[8] Swiss Federal Office of Energy. Energy Strategy 2050 after the Popular Vote, August 2017.

[9] Jakob Moritz Fabian Rager. Urban Energy System Design from the Heat Perspective using mathematical Programming including thermal Storage. PhD thesis, École Polytechnique Fédérale de Lausanne, 2015.

[10] Schweizerischer ingenieur-und architektenverein (SIA). SIA 2024, Raumnutzungsdaten für Energie- und Gebäudetechnik, 2015.

[11] P. Stadler, L. Girardin, and F. Marechal. The Swiss Potential of Model Predictive Control for Building Energy Systems". 2017.

[12] Paul Stadler, Araz Ashouri, and François Maréchal. Model-based optimization of distributed and renewable energy systems in buildings. 120:103–113, 2016.

[13] Paul Stadler, Luc Girardin, Araz Ashour, and François Maréchal. Optimal design and scheduling of building energy systems in smart grids. in submission, 2018.

[14] Paul Stadler, Luc Girardin, Araz Ashouri, and François Maréchal. Contribution of Model Predictive Control in the Integration of Renewable Energy Sources within the Built Environment. Frontiers in Energy Research, 6, May 2018.

[15] Mihai Tomescu, Ils Moorkens, Wouter Wetzels, Lukas Emele, Erik Laes, Erika Meynaerts, European Environment Agency, and European Topic Centre for Air Pollution and Climate Change Mitigation. Renewable energy in Europe 2017: recent growth and knock-on effects. 2017. OCLC: 992693962.

[16] Charles Weinmann and Sahar Pasche. Prévision et justification des consommations d'électricité pour 3 catégories de bâtiment, 2008.